Food Research International 89 (2016) 161–168

Contents lists available at ScienceDirect

Food Research International

journal homepage: www.elsevier.com/locate/foodres

Non-invasive measurement of oxygen diffusion in model foods

Kanishka Bhunia [a], Shyam S. Sablani [a,*], Juming Tang [a], Barbara Rasco [b]

[a] Department of Biological Systems Engineering, Washington State University, P.O. Box 646120, Pullman, WA 99164-6120, United States
[b] School of Food Science, Washington State University, P.O Box 646376, Pullman, WA 99164-6376, United States

ARTICLE INFO

Article history:
Received 23 March 2016
Received in revised form 12 July 2016
Accepted 22 July 2016
Available online 25 July 2016

Keywords:
Agar gel
Fick's law
Hydrodynamic-obstruction model
Numerical solution
Oxydots

ABSTRACT

In this study, we developed a non-invasive method to determine oxygen diffusivity (D_{O_2}) in food gels using an Oxydot luminescence sensor. We designed and fabricated a transparent diffusion cell in order to represent oxygen transfer into foods packaged in an 8-ounce polymeric tray. Oxydots were glued to the sides (*side-dot*) and bottom (*bottom-dot*) of the cell and filled with 1, 2, and 3% (w/v) agar gel as a model food. After deoxygenation, local oxygen concentrations in the gels were measured non-invasively at 4, 12 and 22 °C. Effective oxygen diffusivities in gels (D_{O_2g}) and water (D_{O_2w}) were obtained after fitting experimental data to the analytical solution (data from *side-dot*) and the numerical solution (data from *bottom-dot*) to Fick's second law. Temperature had significant positive influence ($P < 0.05$) on oxygen diffusivity estimated for different medium and analysis methods. The D_{O_2} obtained from both methods were statistically different ($P < 0.05$) at 12 and 22 °C but not at 4 °C. Results show that D_{O_2g} values decreased by 72–92%, compared to D_{O_2w}. Results also show that decreasing the temperature from 22 to 4 °C reduced the D_{O_2w} and D_{O_2g} values by 55–60%. No significant difference ($P > 0.05$) was found between the activation energy (E_a) of water and gels (1–3% w/v) for temperatures ranging from 4 to 22 °C. We used a combined obstruction and hydrodynamic model to explain why D_{O_2g} decreased as gel concentration increased. The method developed in this study can be used to study the oxygen diffusivity in foods.

1. Introduction

The microbial safety and shelf-life of packaged foods are dependent on the level of oxygen in the headspace and food matrices that are packed under Modified Atmospheric Packaging (MAP) (Chaix, Guillaume, & Guillard, 2014) and vacuum packaging. In MAP and in-package thermally processed food, atmospheric oxygen permeates through packaging to the headspace followed by dissolution of headspace oxygen at food surfaces and finally diffusion through food. While oxygen diffuses, food components such as lipids react with oxygen, degrading the nutritional value and overall quality of the food. On the other hand, reducing the oxygen level in packaging usually reduces the growth rate of aerobic microorganisms. However, some oxygen is required to eliminate or delay the growth of anaerobes (Al-Qadiri et al., 2015). Headspace oxygen is often consumed by food while it diffuses through the medium. This results in low oxygen levels at the bottom of the food product, creating a different micro-environment in the food for microbial growth. This scenario is more apparent when foods are solid or highly viscous. Thus, knowledge of oxygen diffusivity (D_{O_2}) and solubility is necessary in order to design packaging and food formulations that yield safe and wholesome foods (Chaix et al., 2014).

The D_{O_2} data are available for a limited number of solid/semisolid foods such as chicken (Baranov, Belichenko, & Shoshenko, 2000; Noriega, Laca, & Diaz, 2010), beef (Zaritzky & Bevilacqua, 1988), agar gels (Adlercreutz, 1986; Hulst, Hens, Buitelaar, & Tramper, 1989; Miller, Nguyen, Rooney, & Kailasapathy, 2003), and yogurt (Miller et al., 2003). However, studies relating D_{O_2} and quality changes are limited. As noted by Chaix, Guillaume, Gontard, and Guillard (2016), D_{O_2} estimated in model minced chicken using Wilke-Chang equation (Noriega et al., 2010) are disputable, since the equation employs the 'viscosity' of solid foods. Solid foods, particularly muscle tissues and gels, are structurally different from fluids (liquid food). Thus, D_{O_2} estimated using viscosity may lead to erroneous results for gels and animal tissues. Additional challenges to estimate D_{O_2} in a solid food involve use of a suitable oxygen quantification method to measure oxygen ingress in the medium as existing techniques are either limited to liquids or invasive in nature.

Food gels are frequently used in jam, jelly, marmalades and yogurts as a gelling and thickening substance. They also have wide range of applications in microbiology including solidifying agent of culture media (1–2%). They are called hydrogels, since their polymeric networks are swollen in large amounts of water. Hydrogels have vast applications in areas of controlled-release drug delivery, therapeutic implants, gel electrophoresis, tissue engineering (Johnson, Berk, Jain, & Deen, 1996; Zhu & Marchant, 2011), agriculture and food packaging (Ullah, Othman, Javed, Ahmad, & Md Akil, 2015).

* Corresponding author.
E-mail address: ssablani@wsu.edu (S.S. Sablani).

http://dx.doi.org/10.1016/j.foodres.2016.07.015
0963-9969/

Oxygen transfer in food involves two simultaneous processes: solubilization of oxygen at food surfaces followed by diffusion. The solubilization process is governed by Henry's law whereas the transient diffusion process is described by Fick's second law. They are described later in the 'Materials and methods' section.

Methodologies to estimate D_{O_2} in food follow three main approaches. The first approach is to monitor pressure decay over time in the headspace of a closed-cell containing food, known as the manometric method. The second approach is known as '*Time-lag*' method. This method uses a permeation system, in which a constant oxygen concentration generated at one side of the food and other side is maintained at either a low-oxygen or an oxygen-free condition. The increase in oxygen concentration or partial pressure at sink-side is monitored over time. The third method is the '*Sorption kinetics*' method, in which O_2 ingress in the food is measured over time and fitted to the analytical solution of Fick's second law, as given by Crank (Crank, 1975). Clark electrode and gas chromatography (GC) techniques are frequently used to detect oxygen. The Clark electrode has an advantage over GC, since it can be used to measure the oxygen content in food and surrounding both. Recently, a rapid and sensitive luminescence quenching method was used to estimate D_{O_2} in water, oils, gels, juices, mashed potato (Penicaud, Guilbert, Peyron, Gontard, & Guillard, 2010), cheese, and cooked ham (Chaix et al., 2016). This method is superior to the Clark electrode method, since oxygen is not consumed during measurement.

The diffusion process may also be affected by physical obstacles such as biopolymer chains or fibers in food. Food gels and meat tissues contain fibrous networks, making them structurally rigid. Gas molecules follow the tortuous path created by polymer chains, slowing down the diffusion process. In the obstruction model, Ogston, Preston, and Wells (1973) followed a phenomenological approach to express the ratio of diffusion coefficient in the gel (D_{O_2g}) to that in the infinite dilution in water (D_{O_2w}) as Eq. (1):

$$\frac{D_{O_2g}}{D_{O_2w}} = exp\left[-\sqrt{\varphi}\frac{r_f + r_s}{r_f}\right] \tag{1}$$

where φ is the polymer volume fraction within the gel, r_f is the radius of the fiber, and r_s is the solute hydrodynamic radius. One limitation of Ogston's model is that it does not consider hydrodynamic effect at higher polymer fraction. Therefore, its applicability is limited to dilute or semi-dilute system of small molecules (Masaro & Zhu, 1999).

The second important theory describing solute movement through hydrogel that is based on the Stokes-Einstein equation is hydrodynamic interaction. One frequently used model proposed by Phillips, Deen, and Brady (1989) is based on the effective medium approach that calculates the frictional factor using Brinkman's equation, as follows (Eq. (2)):

$$\frac{D_{O_2g}}{D_{O_2w}} = \left[1 + r_s/\sqrt{\kappa} + \frac{1}{3}\left(r_s/\sqrt{\kappa}\right)^2\right]^{-1} \tag{2}$$

where κ is the hydraulic permeability. Brady (1994) proposed that long-time hindered diffusion coefficients in fibrous porous media can be expressed as a product of long-time obstruction and short-time hydrodynamic effects. Clague and Phillips (1996) used this concept and combined their hydrodynamic expression with the obstruction term given by Tsai and Strieder (1986) to obtain the following expression (Eq. (3)):

$$\frac{D_{O_2g}}{D_{O_2w}} = \underbrace{\left(1 + \frac{2}{3}\alpha\right)^{-1}}_{\text{Obstruction term}} \underbrace{exp\left(-\pi\varphi^{0.174\ln\left(59.6 r_f/r_s\right)}\right)}_{\text{Hydrodynamic term}} \tag{3}$$

where $\alpha = \varphi\left(\frac{r_f + r_s}{r_f}\right)^2$. This model is applicable for heterogeneous hydrogel with very stiff polymer chains (Amsden, 1998b). Mathematical models based on physical parameters were used to describe the diffusion of solutes such as proteins in agarose (Johnson et al., 1996; Liang et al., 2006), alginate (Amsden, 1998a), and drugs in agarose (Dai et al., 2011). However, to our knowledge, none of the mathematical models based on physical parameters were used to model gas diffusion in hydrogels.

The oxygen diffusivity values for 1–5% agar were reported to vary from 0.197×10^{-9} to 2.7×10^{-9} $m^2\ s^{-1}$ (Adlercreutz, 1986; Hulst et al., 1989; Miller et al., 2003; Penicaud et al., 2010) for temperature ranging between 20 and 30 °C. Gels with higher solid content have lower oxygen diffusivity (Hulst et al., 1989) that further reduces as temperature decreases (Miller et al., 2003). However, D_{O_2} values at refrigerated temperature is still very limited. In this study, we developed a non-invasive method to obtain effective oxygen diffusivity (D_{O_2}) in model foods. We estimated oxygen diffusivity using analytical and numerical solutions of Fick's second law. We also investigated the effect of gel concentration and temperature on D_{O_2}. In addition, we employed mathematical models based on the physical parameters of the model foods to describe the diffusion process in gels.

2. Materials and methods

2.1. Diffusion cells

In this study, a polycarbonate (PC) cell was designed and fabricated to investigate oxygen diffusivity. The PC material was rigid and clear with a thickness of 5 mm. The schematic diagram of the cell is shown in Fig. 1. The design criteria for the diffusion cell was as follows:

- The cell was transparent to the LED sensor probe.
- The cell had an approximate volume of 285.4 cm^3, which is similar to the volume of a standard 8-ounce tray (14.5 cm × 10 cm × 2.5 cm). The maximum height of the food was about 2.0 cm.
- The cell had inner diameter (d) of 12 cm and total height of 2.5 cm. The top lid of the cell had an inlet and an outlet valve. It had six designated screw-holes to securely hold the body of cell together. The cell was supported by two metal rings from the top and bottom of the cell to ensure proper sealing of cells as well as secure handling. An O-ring in the top of the cell was also provided to ensure hermetic seal of the diffusion cell. This cell was used to simulate the diffusion behavior of oxygen in food packed in 8-ounce trays.

2.2. Oxydots and the oxygen analyzer

Oxygen concentration in the medium was measured with a non-invasive oxygen analyzer (Oxysense GEN III 300 series system, OxySense, Las Vegas, NV, U.S.A.). The system had two parts: an oxydot (O2xyDot®, oxygen sensitive dye embedded) and a reader pen with an infrared detector, which was equipped with a data acquisition system (Gen III oxygen analyzer). The Gen III was connected to a computer. The oxydot had a diameter of 5 mm. An oxydot was attached to the internal surface the transparent cell. The other side of the dot was exposed to the medium to react with the oxygen. The dot was excited by blue light from the reader pen. The blue light was absorbed by the dot, while the infrared detector of the reader pen captured the emitted red light from the oxydot. The dynamic quenching process of the dye embedded in oxydot is reversible. The reader pen was also equipped with a fiber optic sensor, facilitating measurement of the local temperature during oxygen measurement. This instrument is over 95% accurate at ambient temperature, and has been validated against the standard oxygen concentration in air. Before measurement, the dots were calibrated against a standard provided by the manufacturer.

2.3. Model foods and medium deoxygenation

Oxygen ingress was monitored for distilled water (DIW) and agar gel. Agar gel (Bacto-agar, BD) was prepared at three concentrations: 1,

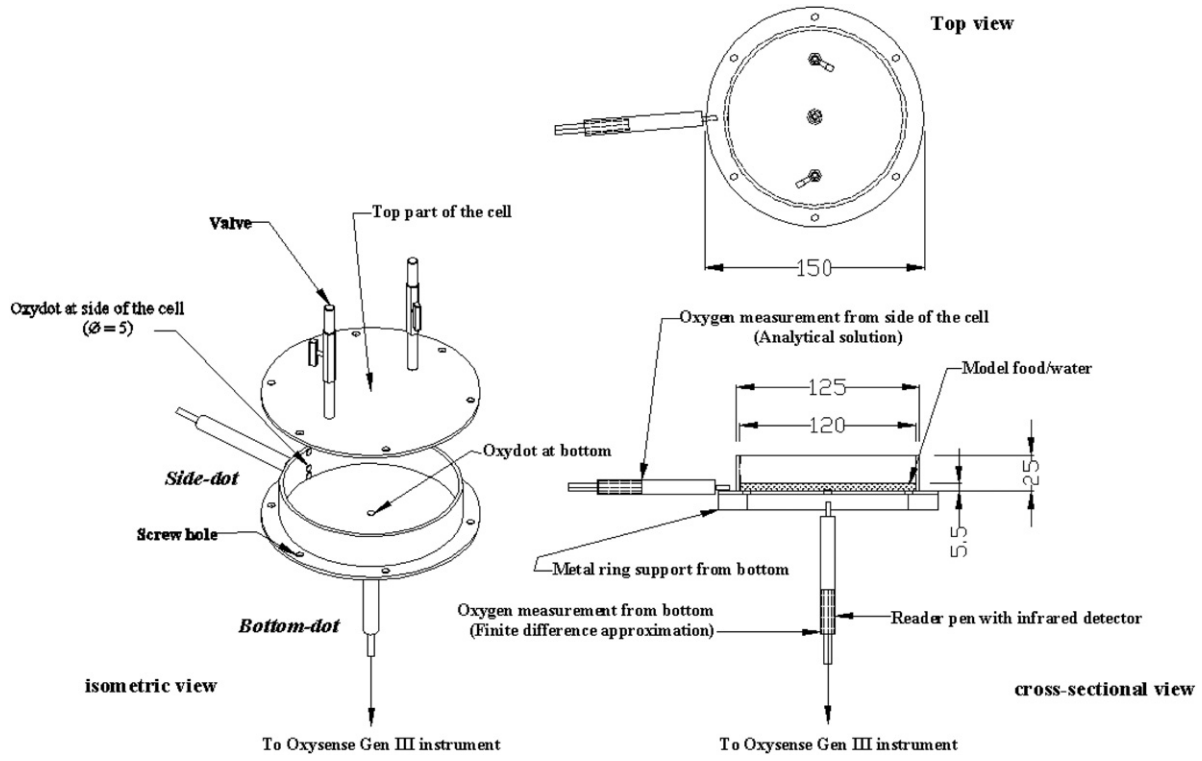

Fig. 1. Design of the transparent diffusion cell (all dimensions are in mm).

2 and 3% (w/v). The desired amount of agar powder was added to hot water (90–95 °C) under continuous stirring. Before filling the test cell with liquid media, the oxydots (5 mm diameter) were attached to the side wall (four locations, just above the bottom) and the bottom of the cell, as shown in Fig. 1. The hot liquid media was then carefully poured into the cell so that the top edge of oxydot was always submerged just below the liquid level (sample thickness = 5.5 ± 0.5 mm). The cell was closed tightly and the valve was opened immediately to allow nitrogen to flow. The drop in oxygen concentration in the medium (water and agar) was monitored with the oxygen sensor. Nitrogen flushing was conducted until the oxygen concentration in the medium reached 5% or less of its saturation value, as indicated by the GEN III oxygen analyzer. The oxygen concentration was checked at all four locations on the side wall and bottom to ensure proper deoxygenation. The valves were closed and disconnected from the N_2 gas source, once it reached an almost oxygen-free environment ($p_{O_2} < 0.5$ mbar).

2.4. Measurement of oxygen ingress

The diffusion cell containing deoxygenated agar gel/water was placed in the incubator (Precision incubator 6.1 cu. ft., Thermo Fisher Scientific, IL) and equilibrated at desired temperature until the sensor showed a stable temperature value. After equilibration, pre-humidified air (21% O_2) was allowed to enter the diffusion cell by opening the valves. Oxygen ingress occurred only from the top of gels/water. Measurements were carried out non-invasively at the inner side-wall (*side-dot*) and bottom of the diffusion cell (*bottom-dot*) (Fig. 1). Data was collected every 120 s until the oxygen concentration reached equilibrium. The partial pressure of oxygen in the cell headspace was measured using another oxydot to ensure a continuous flow of oxygen to the cell. The measurements were carried out for distilled water (DIW) and agar gels at 4 ± 0.5, 12 ± 0.5 and 22 ± 0.5 °C. The thickness of the gel (l) measured at the end of each experiment was 5.5 ± 0.5 mm.

2.5. Mathematical modeling

The increase in oxygen content in the medium was assumed to follow Fick's second law, as in Eq. (4):

$$\frac{\partial C}{\partial t} = D_{O_2} \frac{\partial^2 C}{\partial x^2} \tag{4}$$

where C is the oxygen concentration in the model food (ppb) at any time t (s), and x is the distance in the medium from the gas-medium interface (m). D_{O_2} is the oxygen diffusivity ($m^2\ s^{-1}$) in the medium and assumed to be constant throughout the sample. The medium is considered to be homogenous and isotropic. The diffusion process was assumed to be one-dimensional along the sample thickness.

Initially ($t = 0$), the medium was at uniform concentration (C_0), leading to the following initial condition (Eq. (5))

$$C = C_0, \qquad 0 \le x \le l, \quad t = 0 \tag{5}$$

where l is the thickness of the medium. The air-medium interface was at equilibrium with surrounding oxygen, and the concentration at the interface is the equilibrium oxygen content (C_{eq}) (Dirichlet condition, Eq. (6)):

$$C = C_{eq}, \qquad x = 0, \quad t \ge 0 \tag{6}$$

C_{eq} is the solubility of oxygen in the medium. The solubility term can be correlated to the partial pressure of the surrounding air at equilibrium in the following way (Eq. (7)):

$$C_{eq} = p_{O_2}/H \tag{7}$$

where H is the Henry's law coefficient. The reciprocal of H is the solubility coefficient or partition coefficient ($k_H = 1/H$). At the bottom, no flux

condition exists (Neumann condition, Eq. (8)):

$$\frac{\partial C}{\partial x} = 0, \quad x = l, \quad t \geq 0 \tag{8}$$

Eqs. (4), (5), (6), and (8) were used to obtain the oxygen diffusivity (D_{O_2}) for model foods at different temperatures (4–22 °C) using the aforementioned approach. First, an analytical solution of Eq. (4) was used to model the data obtained from the *side-dot*. Next, an approximate diffusivity value was obtained numerically using the values obtained from the *bottom-dot*. The detail of each approach is explained in the next sections. In general, the oxygen diffusivities in water and agar gel were represented as D_{O_2w} and D_{O_2g}, respectively. D_{O_2g} was the effective diffusivity of oxygen in the agar gel.

2.5.1. Analytical solutions

The cylindrical geometry of water/gels with height l can be simplified as a plane sheet of thickness = l. The thickness of the sheet is much smaller than its diameter ($d/l = 24$), fulfilling the criteria of one dimensional oxygen diffusion from exposed surface, not from the edges. Additionally, the rigid PC diffusion cell is impermeable to gas, imposing no flux condition at the cell edges. The analytical solution to the Fick's second law (Eq. (4)) for one-dimensional diffusion in a plane sheet with thickness l after applying above-mentioned initial and boundary conditions (Eqs. (5), (6), and (8)) is (Crank, 1975) Eq. (9):

$$\frac{C - C_0}{C_{eq} - C_0} = 1 - \sum_{n=0}^{\infty} \frac{8}{(2n+1)^2 \pi^2} e^{-\frac{D_{O_2}(2n+1)^2 \pi^2 t}{4l^2}} \tag{9}$$

The thickness of the medium was 5.5 ± 0.5 mm, a bit more than the diameter of the oxydot (5 mm). Thus, the concentration measured by oxydots on the side wall (*side-dot*) can be approximated as the average oxygen concentration of the bulk medium of thickness l = 5.5 ± 0.5 mm. Measurements were taken in triplicate. The analytical solution was obtained using the non-linear least square technique (*lsqnonlin*) in Matlab (Mathworks, Natic, MA, U.S.A.).

2.5.2. Numerical solutions

In this method, finite difference approximation was implemented to the oxygen concentration measured by oxydot located at the bottom (*bottom-dot*). The domain was discretized with an equal number of grid points so that $\Delta x = \frac{l}{m}$ *and* $m = 50$. The diffusivity values were computed numerically at the 'end grid' point of the medium (at the no-flux boundary). The Eq. (4) was solved with the aforementioned initial (Eq. (5)) and boundary conditions (Eqs. (6) and (8)) using '*pdepe*' solver in Matlab (Mathworks, Natic, MA, U.S.A.). The accuracy of estimated D_{O_2}values was obtained after minimizing the root mean square errors between the experimental and predicted values using Eq. (10):

$$RMSE = \sqrt{\frac{1}{k}\sum_{t=1}^{k}(C_{et} - C_{pt})^2} \tag{10}$$

where C_{et} and C_{pt} are the experimental and predicted oxygen content at time t and k is the number of observations.

2.6. Temperature dependence of oxygen diffusivity

The Arrhenius-type equation was used to describe the temperature dependency of oxygen diffusivity in model foods as follows (Eq. (11)):

$$D_{O_2} = D_0 e^{-\left(\frac{E_a}{RT}\right)} \tag{11}$$

where D_0 is the pre-exponential factor, E_a is the activation energy for molecular diffusion, T is the absolute temperature (K), and R is the universal gas constant (8.314 J mol^{-1} K^{-1}).

2.7. Modeling the diffusion based on physical parameters of model foods

To obtain a better understanding of oxygen diffusivity in fibrous network, we compared the experimental data and theoretical representation of oxygen transport. The model, therefore, will help in predicting the diffusivity of oxygen considering physical parameters of gel. The first step in the modeling was to determine the solute hydrodynamic radius using the Stokes-Einstein equation (Eq. (12)):

$$r_s = \frac{k_B T}{f \pi \eta D_{O_2 w}} \tag{12}$$

where k_B is the Boltzmann's constant, T is the absolute temperature, η is the viscosity of solvent (water) at T, f is 4 for solutes of size approaching to solvent size (water) or 6 for solutes greater than solvent molecule size. To calculate the polymer volume fraction, φ, Eq. (13) (Johnson, Berk, Jain, & Deen, 1995) was used:

$$\varphi = \frac{C_{agar}}{\omega_{agar} \rho_{agar}} \tag{13}$$

where C_{agar} is the mass fraction of agar, $\omega_{agar} = 0.625$ is the mass fraction of agarose in the hydrogel fiber (Johnson et al., 1995), and ρ_{agar} is the density of dry agarose powder (1.67 g ml^{-1}) (Laurent, 1967). Brady (1994) suggested that the influence of obstruction and hydrodynamic interaction on diffusivity of hydrogels has two multiplicative factors. Using this approach, Ogston's obstruction term can be combined with the hydrodynamic term of Clague and Phillips model (Eq. (3)) to obtain the following equation (Eq. (14)):

$$\frac{D_{O_2 g}}{D_{O_2 w}} = \underbrace{exp\left[-\sqrt{\varphi}\frac{r_f + r_s}{r_f}\right]}_{\text{Obstruction term}} \underbrace{exp\left(-\pi\varphi^{0.174 \ln\left(59.6 r_f / r_s\right)}\right)}_{\text{Hydrodynamic term}} \tag{14}$$

In this study, we used the developed model (Eq. (14)) to predict D_{O_2g} and to compare it with existing models by Ogston (Eq. (1)) as well as Clague and Phillips (Eq. (3)). Agarose hydrogel fibers have a bimodal distribution of α-helix chains; 13% have a radius of 4.5 nm and 87% have a radius of 1.5 nm, resulting in an r_f value of 1.9 nm (Amsden, 1998b). Since agar and agarose exhibit similar physical properties, we assume that the agar gels contain fiber chains with r_f = 1.9 nm. A brief experimental sequence was presented in Fig. 2.

2.8. Statistical analysis

A completely randomized design (CRD) with an ANCOVA test was performed to conduct the statistical test. Temperature was considered as a quantitative factor and set as a covariate whereas medium and analysis method were considered as qualitative factor for the analysis. Therefore, the test was 2-way ANOVA with single covariate. The analyzed data were presented as mean value and standard deviation (SD) from three replicate samples of each treatment combination. The oxygen uptake data were collected for a total number (N) of 72 samples (n = 3 replicates for each treatment combination). The residuals were tested for normality (Shapiro-wilk test) (Granato, Calado, & Jarvis, 2014). The assumption of equal variance was tested by investigating the residual plot. A pairwise comparison (Tukey's test) was performed for agar percentage and analysis methods at three temperature levels (4, 12, and 22 °C) after confirming a significant overall F test at α = 0.05. A statistical software SAS 9.2 (SAS Inst. Inc., Cary, NC, U.S.A.) was used to conduct the data analysis.

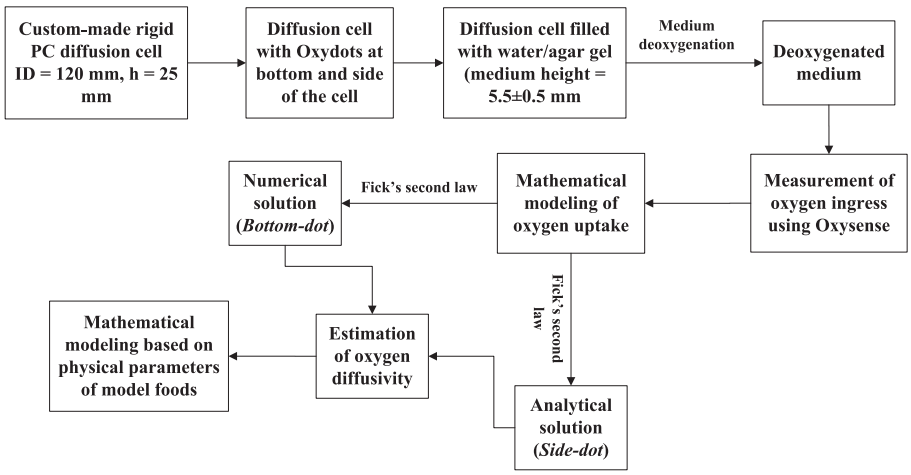

Fig. 2. Experimental sequence of the present study to estimate oxygen diffusivity in water and agar gels.

3. Results and discussion

3.1. Comparison between analytical and numerical solutions

Our statistical analysis showed that the residuals were normally distributed (P value from Shapiro-Wilk test >0.05). A random distribution of residuals around zero line in the residual plot was observed, indicating the assumption of constant variance is valid.

The analytically estimated values of D_{O_2w} were $2.20 \pm 0.1 \times 10^{-9}$, $1.55 \pm 0.05 \times 10^{-9}$, and $1.24 \pm 0.05 \times 10^{-9}$ $m^2\ s^{-1}$ at 22, 12, and 4 °C, respectively (Table 1). The corresponding D_{O_2w} values, when obtained numerically (finite difference approximation), were $2.00 \pm 0.08 \times 10^{-9}$, $1.50 \pm 0.07 \times 10^{-9}$, and $1.17 \pm 0.07 \times 10^{-9}$ $m^2\ s^{-1}$. A significant interaction between temperature (covariate) and analysis method ($P < 0.05$) was found, indicating that slopes of the regression lines across the methods are different (Table 2). Therefore, a comparison between two mediums must be performed at a particular value of covariate (Ott & Longnecker, 2008). The D_{O_2} from analytical method were significantly higher than numerical values ($P < 0.05$) at 12 and 22 °C, however, no significant difference ($P > 0.05$) was found at 4 °C (Table 3). The measured oxygen concentration from the *bottom-dot* had a distinct initial time-lag that was not apparent for the *side-dot* (Fig. 3).

It is important to consider the applicability of both methods in order to estimate the D_{O_2} in water and food gels. Note that, the D_{O_2} from analytical method were ≤10% higher than the numerical values for each treatment combinations (Table 1). Although the D_{O_2w} estimated from both methods were statistically different from each other (except at 4 °C), both values fell within the range of previously reported values (Han & Bartels, 1996; Penicaud et al., 2010). For example, the reported values of D_{O_2w} were 2.48×10^{-9} $m^2\ s^{-1}$ at 20 °C (Penicaud et al., 2010), and 1.85×10^{-9} $m^2\ s^{-1}$ at 22 °C (Han & Bartels, 1996). Therefore, it can be stated that both methods are equally applicable for obtaining the D_{O_2} in the liquid and biopolymer food gels. The analytical solution followed in *side-dot* is sensitive to the thickness of the medium. A thicker medium may cause an incorrect estimation of D_{O_2}, since the measured oxygen content by oxydot would not represent the total bulk medium. Therefore, the precise thickness of 5.5 ± 0.5 mm must be maintained, so that the edge of oxydot is immersed just below the surface. Nevertheless, the *side-dot* method is very useful for determining oxygen content at one or more locations in a food along its height. Multiple oxydots can be used at desired locations with in a food to measure oxygen content. The data obtained can be further used to study the oxidation or microbial growth in foods.

3.2. Effects of agar concentration on oxygen diffusivity

The oxygen diffusivity in DIW (D_{O_2w}) obtained from the analytical solution was $2.20 \pm 0.10 \times 10^{-9}$ $m^2\ s^{-1}$ at 22 ± 1 °C. The estimated D_{O_2} in 1–3% agar gels (D_{O_2g}) at 22 ± 1 °C ranged from $1.98 \pm 0.05 \times 10^{-9}$ to $1.60 \pm 0.04 \times 10^{-9}$ $m^2\ s^{-1}$ (Table 1). The interaction between medium and temperature was highly significant ($P = 0.0025 < 0.05$), indicating that at least one of the regression lines (intercepts and slopes) differ significantly across the medium groups (Table 2). To evaluate this, a pairwise contrast was performed. The contrast for comparison indicated that water (0% agar) differed in slope from 2 and 3% agar but not from 1% agar, while 1% agar differed in slope from 3% agar but not from 2% agar, and 2% agar did not differ in slope from 3% agar (Table 2). Our analysis also indicated that the estimated mean values of D_{O_2} were the highest in water and significantly decreased ($P < 0.05$) with increasing agar concentration (Table 3).

Agar readily dissolves in hot water (above 85 °C) and forms a weak to strong gel (depending on concentration) upon cooling to ambient temperature. The structure of agar gel has a three-dimensional network

Table 1
Oxygen diffusivity values in water and agar gels (1–3%) at 4, 12 and 22 °C.

Temperature, °C	Analysis method*	Oxygen diffusivity, $D_{O_2} \times 10^9$ $m^2\ s^{-1}$			
		Medium			
		Water	1% agar	2% agar	3% agar
4 ± 0.5	Analytical	1.24 ± 0.05	1.16 ± 0.0	1.02 ± 0.07	0.92 ± 0.03
	Numerical	1.17 ± 0.07	1.08 ± 0.03	0.94 ± 0.05	0.88 ± 0.02
12 ± 0.5	Analytical	1.55 ± 0.05	1.38 ± 0.08	1.25 ± 0.03	1.11 ± 0.10
	Numerical	1.50 ± 0.07	1.31 ± 0.02	1.21 ± 0.01	1.10 ± 0.07
22 ± 0.5	Analytical	2.20 ± 0.10	1.98 ± 0.05	1.76 ± 0.04	1.60 ± 0.04
	Numerical	2.00 ± 0.08	1.83 ± 0.05	1.64 ± 0.02	1.50 ± 0.04

*Analytical: oxydot at inner side of wall of diffusion cell; Numerical: oxydot at bottom of the diffusion cell. Diffusivity values are presented as the mean ± SD.

Table 2
Comparison of slopes of lines for factors when temperature is a linear predictor.

Methods	Grouping
Analytical	A
Numerical	B
Medium	**Grouping**
Water	A
1% agar	AB
2% agar	BC
3% agar	C

Groups with different letters are significantly different from each other ($P < 0.05$).

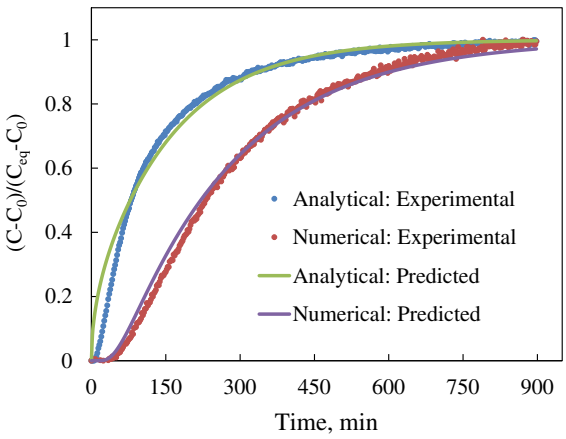

Fig. 3. Representative plot of normalized oxygen concentration over time obtained from analytical and numerical solutions for 2% (w/v) agar gel at 4 °C. (Analytical: *side-dot*; Numerical: *bottom-dot*).

that is made up of stiff biopolymer chains. The presence of polymer fibers in the structure increases the mean free path for the diffusion of oxygen molecules. The D_{O_2g} in 1% agar gel at 22 ± 1 °C was 1.98×10^{-9} m^2 s^{-1}, which was 90% of that in the DIW. This result shows good agreement with the earlier reported value, in which D_{O_2}in 1% agar gel was ~89% of that in pure water at 20 °C (Penicaud et al., 2010). The D_{O_2} in 1% agar gel was 87–92% of D_{O_2w} at temperatures ranging from 4 to 22 °C. These values further decreased to 80–81% and 72–75% for 2 and 3% agar gels, respectively. Increasing the agar amount created a denser network, increased the tortuosity, and lowered the oxygen diffusivity. Hulst et al. (1989) found that D_{O_2} in 2% (w/v) agar was 85% of that in pure water, which is slightly lower than our results. However, reported values of D_{O_2} is 2% (w/v) agar was 70% (Sato & Toda, 1983) and 77% of $D_{O_{2w}}$ (Adlercreutz, 1986) at 30 °C, lower than our results.

3.3. Temperature effects on oxygen diffusivity

Results for the analytically estimated value of D_{O_2w} ranged from $1.24 \pm 0.05 \times 10^{-9}$ to $2.20 \pm 0.10 \times 10^{-9}$ m^2 s^{-1} at 4–22 °C (Table 1). Temperature had a significant influence on D_{O_2} obtained for medium ($P_{\text{medium} \times \text{temperature}} = 0.0025 < 0.05$) and analysis method ($P_{\text{method} \times \text{temperature}} = 0.044 < 0.05$). Note that, the influence of temperature on $D_{O_2}$was more pronounced for different medium compared to analysis method. The D_{O_2w} significantly increased ($P < 0.05$) with temperature increased from 4 °C to 12 °C (1.25–1.28 fold) and 22 °C (1.71–1.77 fold). For agar gels, the mean D_{O_2g} values at 4 °C were 1.16×10^{-9}, 1.02×10^{-9} and 0.92×10^{-9} m^2 s^{-1} for 1%, 2%, and 3% (w/v) agar, respectively. Increasing the temperature from 4 to 22 °C, significantly increased the D_{O_2g} by 1.7–1.76, 1.72–1.74, and 1.70–1.73 times for 1%, 2%, and 3% (w/v) agar gel, respectively. Thus, temperature had a positive influence on oxygen diffusivity in water and in food gels. The average values of solubility coefficient (k_H) for water were 1.34×10^{-8}, 1.93×10^{-8}, and 2.16×10^{-8} mol kg^{-1} Pa^{-1} at 22, 12, and 4 °C, respectively. Sander (2015) reported the solubility coefficient for water at 25 °C range from 1.2×10^{-8} – 1.3×10^{-8} mol kg^{-1} Pa^{-1}. The k_H values increased with decreasing temperature, indicating that oxygen dissolves more as temperature falls.

Table 3
Comparison of least square mean values of oxygen diffusivity.

Methods	Oxygen diffusivity, $D_{O_2} \times 10^9$ m^2 s^{-1}		
	Temperature, °C		
	4	12	22
Analytical	1.03 [a]	1.40 [a]	1.85 [a]
Numerical	0.99 [a]	1.32 [b]	1.72 [b]
Medium	**4**	**12**	**22**
Water	1.17 [a]	1.57 [a]	2.07 [a]
1% agar	1.08 [a]	1.43 [b]	1.87 [b]
2% agar	0.95 [bc]	1.27 [c]	1.67 [c]
3% agar	0.86 [c]	1.15 [d]	1.52 [d]

Groups with different letters are significantly different from each other ($P < 0.05$). Values were compared along the column.

It is well-known that the molecular diffusion process is highly influenced by temperature. Oxygen molecules have more energy at higher temperatures, facilitating the diffusion process. It is important to note that the increase in D_{O_2} in agar gels (1.70–1.73 fold) is similar to that of water (1.71–1.77 fold) as temperature increases from 4 to 22 °C. This indicates that the diffusion of oxygen molecules occurs mainly through water-filled regions of the polymer networks, although biopolymer fibers in the gel hinder the diffusion process, resulting in low D_{O_2} in gels.

In the study, the reported values of D_{O_2w} at 22 °C ranged from 2.11×10^{-9} to 2.25×10^{-9} m^2 s^{-1} (Himmelblau, 1964; Ju & Ho, 1989). In the present study, the obtained D_{O_2w} at 22 °C was 2.00×10^{-9} (numerical) and 2.20×10^{-9} m^2 s^{-1} (analytical). Note that even in the simplest medium, the process of obtaining diffusivity is sensitive to temperature. For example, diffusion in liquid samples is often accompanied by convection due to temperature fluctuation and improper handling. This often results in higher D_{O_2}. Han and Bartels (1996) determined D_{O_2w} at temperatures ranging from −0.5 to 95 °C using the Taylor dispersion technique. They proposed an interpolation formula as follows (Eq. (15)):

$$\log_{10} D_{O_2w} = -4.41 + 773.8/T - (506.4/T)^2 \quad (15)$$

where D_{O_2w} is in cm^2 s^{-1}; T in K. Using Eq. (15), calculated D_{O_2w} values at 4, 12, and 22 °C would be 1.10×10^{-9}, 1.41×10^{-9}, and 1.85×10^{-9} m^2 s^{-1}, respectively. These are close to the values obtained from the numerical solution (Table 1).

In the present study, the D_{O_2} values were used to determine the activation energy (E_a) of oxygen diffusion in water and agar gels at temperatures ranging from 4 to 22 °C. The activation energy for oxygen diffusion in water was 21.4 ± 1.4 kJ mol^{-1}. This value for water was a bit higher than E_a = 19.5 kJ mol^{-1}, which was calculated using the D_{O_2w}values predicted from Eq. (15) (Han & Bartels, 1996) for a similar temperature range (4–22 °C). The activation energy values for diffusion of oxygen molecules in 1%, 2%, and 3% agar gel were 20.3 ± 1.4, 21.7 ± 0.8, and 20.5 ± 0.9 kJ mol^{-1}, respectively. These values compare well with reported value for 5% (w/w) gelatin (E_a = 20.3 kJ mol^{-1}), calculated for temperature range of 10–25 °C (Simpson, Almonacid, Acevedo, & Cortes, 2004). Note that these values did not differ significantly ($P > 0.05$) from E_a of D_{O_2}in water, indicating that the presence of small amounts of agar (1–3% w/v) in water does not significantly affect the E_a. Agar gels contain a major amount of water trapped between three-dimensional polymer networks. Therefore, the D_{O_2}in gels decreased primarily because the presence and interaction of polymer

chains hindered diffusion. Cox and Dunn (1986) found a similar result on the effect of temperature on oxygen diffusion in silica-filled linear poly (dimethyl siloxane). They concluded that the activation energy for D_{O_2} remained the same for small silica concentrations (up to 5 wt%).

3.4. Modeling the diffusion based on physical parameters of model foods

The oxygen diffusivities in gels relative to D_{O_2w} ($D_r = D_{O_2g}/D_{O_2w}$) were predicted from Ogston (Eq. (1)), Clague and Philips (Eq. (3)), and present model (Eq. (14)) for different agar concentration at 22 °C and plotted in Fig. 4. The plotting indicates that Ogston's obstruction model provides good agreement at $\varphi = 0.0097$ (calculated using Eq. (13)), beyond which the model over-predicted the D_r. Muhr and Blanshard (1982) reported that the Ogston model overestimated D_r with increasing φ for solute molecules of moderate size ($r_s \sim r_f$). The low diffusivity values of such solutes (urea, sucrose, glucose) in gels (agar, polyacrylamide gels) cannot be explained only by obstruction theory (Muhr & Blanshard, 1982). They also postulated that enhanced frictional drag (hydrodynamic effect) by polymer on the moderately size molecules caused such a low value of D_{O_2g}.

In an another study on diffusion of spheres in crowded rods, Kang et al. (2005) found that the hydrodynamic effect becomes more significant for diffusing solutes with a diameter that is smaller than the rod diameter. Similar observations were made by Zhang and Amsden (2006), who found that the obstruction-scaling model overestimates the effective diffusivity of smaller molecule (vitamin B_{12}, $r_s = 0.87$ nm) in semi-dilute polymer solution. This is because hydrodynamic interactions were not considered in the obstruction-scaling model.

Our results show that the size of oxygen molecules ($r_s = 0.175$ nm) was much smaller than the fiber radius ($r_f = 1.9$ nm). However, it is important to determine whether this finding for semi-dilute polymer solutions (Zhang & Amsden, 2006) is applicable to gels. Johnson et al. (1996) concluded that the obstruction and hydrodynamic factors in semi-dilute polymer solutions would be very similar to the gel (not dilute) if the size of the diffusing molecule was smaller than the separation between polymer chains ($r_s < \kappa^{1/2}$). Using this theory, the value of κ was calculated from following correlation (Eq. (16)) (Jackson & James, 1986):

$$\frac{\kappa}{r_f^2} = -\frac{3}{20\varphi}(\ln\varphi + 0.931) \tag{16}$$

The calculated value of $\kappa^{1/2}$ varied from 14.3 nm ($\varphi = 0.0097$) to 7.0 nm ($\varphi = 0.03$) which is much higher than r_s of oxygen which is 0.173 nm ($r_s << \kappa^{1/2}$). Therefore, the obstruction and hydrodynamic effect on solute molecule in agar gels would be similar to the semi-dilute polymer solutions. Thus, the results from Zhang and Amsden (2006) for smaller diffusants in a semi-dilute polymer solution is also applicable to our study. This suggests that the hydrodynamic effect cannot be neglected to explain the diffusivity of small oxygen molecule in gels. Furthermore, the macroscopic diffusivities in gels (D_{O_2g}) was estimated from experimental data that are long time scales (measurement time was 5 s at 120 s interval). At short time scales (several microseconds), hydrodynamic interactions dominate, whereas both obstruction and hydrodynamic effects are important at long time scales (Clague & Phillips, 1996). Hence, the diffusion phenomenon in gel is influenced by both steric obstruction and hydrodynamic interactions.

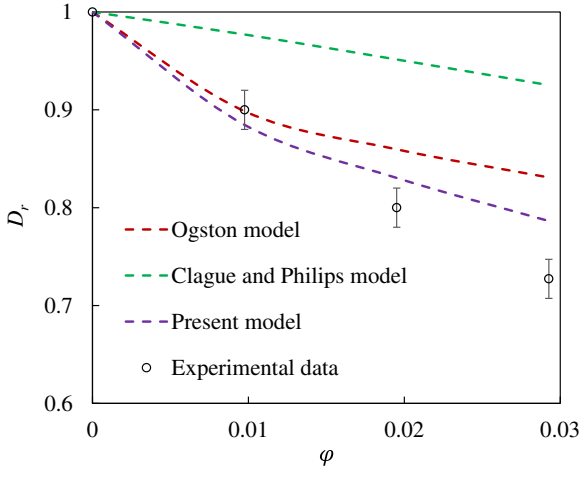

Fig. 4. Comparison between experimental data (*side-dot*) and mathematical models by Ogston (Eq. (1)), Clague and Philips (Eq. (3)), and present work (Eq. (14)) for oxygen diffusivity in agar gels at 22 °C.

The predicted value of D_r using the combined model of Clague and Philips (Eq. (3)) exhibited large deviation from the experimental data (Fig. 4). However, when the hydrodynamic term from Clague and Philips model was combined with Ogston obstruction effect, the resulting model (Eq. (14)) showed a better fit to the experimental observations. This result was valid at two other temperatures (4 and 12 °C, data not presented). The value of the obstruction term in the present model (Eq. (14)) at $\varphi = 0.0097$ was 0.90, which was close to the experimental value. However, the value predicted from Clague and Philips model was 0.99, which is higher than the value we observed. This may lead to overestimation of oxygen diffusivity in gels. Clague and Philips model was proven to provide good estimation of diffusivity of large molecules in agarose hydrogels (Liang et al., 2006), but may not be suitable for small molecules. Thus, the combined obstruction and hydrodynamic model that we proposed can better predict the oxygen diffusivity in agar gels.

4. Conclusions

In this study, we developed and tested a non-invasive technique to estimate oxygen diffusivity in water and food gels. We employed two methodologies (analytical and numerical) to measure oxygen content in the medium. The D_{O_2} values estimated from the numerical solution (finite different approximation) were significantly lower ($P < 0.05$) than the analytical solution (within 10%) at 12 and 22 °C. However, regardless of the methodology used, the obtained D_{O_2w} values were in accordance with previously reported values. This indicates that both methods are suitable for determining the oxygen content in foods. The *side-dot* approach is useful when knowledge of oxygen content at different locations (along height) in a food is required.

The addition of agar significantly decreased ($P < 0.05$) the D_{O_2} to 72–92% of D_{O_2w} for 3–1% (w/v) agar gels. Temperature had a positive impact on D_{O_2} in water and gels. However, the activation energy for water (21.4 ± 1.4 kJ mol^{-1}) and agar gels (20.3 ± 1.4–21.7 ± 0.8 kJ mol^{-1}) were similar for the temperature range (4–22 °C) in this study. The oxygen molecules followed a tortuous path around the agar-biopolymer fibers, increasing the mean path for diffusion and lowering the D_{O_2} in agar gels. The obstruction-hydrodynamic model effectively described the oxygen diffusivity in gels. This new method can be used to measure oxygen diffusion in food to describe microbial growth and oxidation processes.

Nomenclatures and acronyms

C_0 initial concentration of oxygen in the medium, ppb
C oxygen content at any time, ppb
C_{agar} concentration of agar, w/v
DIW distilled water
C_{eq} equilibrium oxygen content, ppb
H Henry's law coefficient
C_{et} experimental oxygen content, ppb
PC polycarbonate
C_{pt} predicted oxygen content, ppb
RMSE root mean square error

D_{O_2} oxygen diffusivity, $m^2\ s^{-1}$
m number of grids in sheet geometry
D_{O_2g} oxygen diffusivity in gel, $m^2\ s^{-1}$
O_2 oxygen
D_{O_2w} oxygen diffusivity in water, $m^2\ s^{-1}$
k number of experimental data
D_0 pre-exponential factor
R universal gas constant, J $mol^{-1}\ K^{-1}$
D_r relative diffusivity
RH relative humidity
E_a activation energy, kJ mol^{-1}
t time, s
k_B Boltzmann's constant
T Temperature, K
k_H solubility or partition coefficient
d diameter of the diffusion cell, cm
p_{O_2} partial pressure of oxygen, mbar
f constant in Stokes-Einstein equation
r_f radius of the fiber, nm
l thickness of the medium, m
r_s Hydrodynamic radius of solute, nm
x distance between interface and any arbitrary point in the medium, m
ρ_{agar} density of dry agarose powder, g ml^{-1}
η viscosity of water
ω_{agar} mass fraction of agarose in the hydrogel fiber
κ hydraulic permeability, nm^2
Δx size of grids in plane sheet geometry
φ polymer volume fraction within gel

Acknowledgements

This work was partially funded by USDA-NIFA Food Safety grant #2011-68003-20096 and Improving Food Quality grant #2016-67017-24597.

References

Adlercreutz, P. (1986). Oxygen supply to immobilized cells: 5. Theoretical calculations and experimental data for the oxidation of glycerol by immobilized Gluconobacter oxydans cells with oxygen or p-benzoquinone as electron acceptor. *Biotechnology and Bioengineering*, *28*(2), 223–232.

Al-Qadiri, H., Sablani, S. S., Ovissipour, M., Al-Alami, N., Govindan, B., & Rasco, B. (2015). Effect of oxygen stress on growth and survival of *Clostridium perfringens*, *Campylobacter jejuni*, and *Listeria monocytogenes* under different storage conditions. *Journal of Food Protection*, *78*(4), 691–697.

Amsden, B. (1998a). Solute diffusion in hydrogels. An examination of the retardation effect. *Polymer Gels and Networks*, *6*(1), 13–43.

Amsden, B. (1998b). Solute diffusion within hydrogels. Mechanisms and models. *Macromolecules*, *31*(23), 8382–8395.

Baranov, V. I., Belichenko, V. M., & Shoshenko, C. A. (2000). Oxygen diffusion coefficient in isolated chicken red and white skeletal muscle fibers in ontogenesis. *Microvascular Research*, *60*(2), 168–176.

Brady, J. (1994). Hindered diffusion. *American Institute of Chemical Engineers, annual meeting, November 13–18*. San Francisco: CA.

Chaix, E., Guillaume, C., & Guillard, V. (2014). Oxygen and carbon dioxide solubility and diffusivity in solid food matrices: A review of past and current knowledge. *Comprehensive Reviews in Food Science and Food Safety*, *13*(3), 261–286.

Chaix, E., Guillaume, C., Gontard, N., & Guillard, V. (2016). Performance of a non-invasive methodology for assessing oxygen diffusion in liquid and solid food products. *Journal of Food Engineering*, *171*, 87–94.

Clague, D. S., & Phillips, R. J. (1996). Hindered diffusion of spherical macromolecules through dilute fibrous media. *Physics of Fluids*, *8*(7), 1720–1731.

Cox, M. E., & Dunn, B. (1986). Oxygen diffusion in poly(dimethyl siloxane) using fluorescence quenching II. Filled samples. *Journal of Polymer Science Part A: Polymer Chemistry*, *24*(10), 2395–2400.

Crank, J. (1975). *The mathematics of diffusion*. Oxford university press.

Dai, H., Wu, J., Wang, Y., Tan, S., Liang, S., Jiang, B., ... Xu, J. (2011). Diffusion of levofloxacin mesylate in agarose hydrogels monitored by a refractive-index method. *Journal of Applied Polymer Science*, *122*(5), 3000–3006.

Granato, D., de Araújo Calado, V. M., & Jarvis, B. (2014). Observations on the use of statistical methods in food science and technology. *Food Research International*, *55*, 137–149.

Han, P., & Bartels, D. M. (1996). Temperature dependence of oxygen diffusion in H_2O and D_2O. *Journal of Physical Chemistry*, *100*(13), 5597–5602.

Himmelblau, D. (1964). Diffusion of dissolved gases in liquids. *Chemical Reviews*, *64*(5), 527–550.

Hulst, A. C., Hens, H. J. H., Buitelaar, R. M., & Tramper, J. (1989). Determination of the effective diffusion coefficient of oxygen in gel materials in relation to gel concentration. *Biotechnology Techniques*, *3*(3), 199–204.

Jackson, G. W., & James, D. F. (1986). The permeability of fibrous porous media. *The Canadian Journal of Chemical Engineering*, *64*(3), 364–374.

Johnson, E. M., Berk, D. A., Jain, R. K., & Deen, W. M. (1995). Diffusion and partitioning of proteins in charged agarose gels. *Biophysical Journal*, *68*(4), 1561–1568.

Johnson, E. M., Berk, D. A., Jain, R. K., & Deen, W. M. (1996). Hindered diffusion in agarose gels: Test of effective medium model. *Biophysical Journal*, *70*(2), 1017–1023.

Ju, L. K., & Ho, C. S. (1989). Oxygen diffusion coefficient and solubility in n-hexadecane. *Biotechnology and Bioengineering*, *34*(9), 1221–1224.

Kang, K., Gapinski, J., Lettinga, M. P., Buitenhuis, J., Meier, G., Ratajczyk, M., ... Patkowski, A. (2005). Diffusion of spheres in crowded suspensions of rods. *Journal of Chemical Physics*, *122*(4).

Laurent, T. C. (1967). Determination of the structure of agarose gels by gel chromatography. *Biochim Biophys Acta*, *136*(2), 199–205.

Liang, S., Xu, J., Weng, L., Dai, H., Zhang, X., & Zhang, L. (2006). Protein diffusion in agarose hydrogel in situ measured by improved refractive index method. *Journal of Control Release*, *115*(2), 189–196.

Masaro, L., & Zhu, X. X. (1999). Physical models of diffusion for polymer solutions, gels and solids. *Progress in Polymer Science*, *24*(5), 731–775.

Miller, C. W., Nguyen, M. H., Rooney, M., & Kailasapathy, K. (2003). Novel apparatus to measure oxygen diffusion in gel-type foods. *Food Australia*, *55*(9), 432–435.

Muhr, A. H., & Blanshard, J. M. V. (1982). Diffusion in gels. *Polymer*, *23*(7), 1012–1026.

Noriega, E., Laca, A., & Diaz, M. (2010). Development of a structure-based model for the competitive growth of *Listeria innocua* in minced chicken breasts. *Internationa Journal of Food Microbiology*, *142*(1–2), 44–52.

Ogston, A. G., Preston, B. N., & Wells, J. D. (1973). On the transport of compact particles through solutions of chain-polymers. *Proceedings of the Royal Society of London A: Mathematical, Physical and Engineering Sciences*, *333*(1594), 297–316.

Ott, R. L., & Longnecker, M. T. (2008). *An introduction to statistical methods and data analysis* (6th ed.) Cengage Learning. (Chapter 16).

Penicaud, C., Guilbert, S., Peyron, S., Gontard, N., & Guillard, V. (2010). Oxygen transfer in foods using oxygen luminescence sensors: Influence of oxygen partial pressure and food nature and composition. *Food Chemistry*, *123*(4), 1275–1281.

Phillips, R. J., Deen, W. M., & Brady, J. F. (1989). Hindered transport of spherical macromolecules in fibrous membranes and gels. *AICHE Journal*, *35*(11), 1761–1769.

Sander, R. (2015). Compilation of Henry's law constants (version 4.0) for water as solvent. *Atmospheric Chemistry & Physics*, *15*(8).

Sato, K., & Toda, K. (1983). Oxygen-uptake rate of immobilized growing candida-lipolytica. *Journal of Fermentation Technology*, *61*(3), 239–245.

Simpson, R. J., Almonacid, S. F., Acevedo, C. A., & Cortes, C. A. (2004). Simultaneous heat and mass transfer applied to non-respiring foods packed in modified atmosphere. *Journal of Food Engineering*, *61*(2), 279–286.

Tsai, D. S., & Strieder, W. (1986). Effective conductivities of random fiber beds. *Chemical Engineering Communications*, *40*(1–6), 207–218.

Ullah, F., Othman, M. B., Javed, F., Ahmad, Z., & Md Akil, H. (2015). Classification, processing and application of hydrogels: A review. *Mater Sci. Eng. C. Mater. Biol. Appl.*, *57*, 414–433.

Zaritzky, N. E., & Bevilacqua, A. E. (1988). Oxygen diffusion in meat tissues. *International Journal of Heat and Mass Transfer*, *31*(5), 923–930.

Zhang, Y., & Amsden, B. G. (2006). Application of an obstruction-scaling model to diffusion of vitamin B-12 and proteins in semidilute alginate solutions. *Macromolecules*, *39*(3), 1073–1078.

Zhu, J., & Marchant, R. E. (2011). Design properties of hydrogel tissue-engineering scaffolds. *Expert Review in Medical Devices*, *8*(5), 607–626.